Ultraviolet Reflection Spectrum of Cubic CdS

MANUEL CARDONA*
Department of Physics, Brown University, Providence, Rhode Island
AND
MARTIN WEINSTEIN† AND G. A. WOLFF†
Tyco Laboratories, Waltham, Massachusetts
(Received 24 May 1965)

The normal-incidence reflection spectrum of cubic CdS has been measured for photon energies between 2 and 22 eV. The samples were prepared by epitaxial deposition on the {1$\bar{1}$1} "As face" of GaAs. The lowest direct absorption edge produces a reflection peak at 2.50 eV at room temperature. The E_1 peak (at 5.49 eV) does not show the splitting characteristic of hexagonal (wurtzite-type) material. The F_1 peak previously reported for wurtzite-type CdS at 7.12 eV is absent in cubic CdS. All other features of the reflection spectra of cubic and hexagonal CdS are very similar. The mixed cubic-hexagonal nature of CdS films deposited on the {1$\bar{1}$1} "P face" of GaP is easily detected with the help of the reflection spectrum: The split component of the E_1 peak and the F_1 peak appear less intensely than in pure hexagonal CdS. The preparation and epitaxy of cubic and hexagonal CdS films are described and interpreted.

INTRODUCTION

MEASUREMENTS of the reflection spectra of diamond, zincblende, and wurtzite-type materials have yielded much useful information about their energy band structures.[1] It has been shown that the reflection spectra[2] and thus the band structures[3] of materials with wurtzite structure are very similar to those the materials would have when crystallized in the zincblende structure. Most of the evidence in favor of the similarity between zincblende and wurtzite reflection spectra is, however, rather circumstantial, since only measurements for one material (ZnS) crystallized in both the zincblende and the wurtzite structure have been reported. In this paper, we present measurements on cubic and hexagonal CdS prepared by epitaxial deposition on cubic GaAs and GaP substrates. It is shown that the energy gap of cubic CdS is nearly the same as that of the hexagonal material. The previous interpretation of the reflection data of hexagonal CdS is confirmed by measurements on the cubic material: The E_1 reflection peak, split in wurtzite because of the hexagonal symmetry, appears as a singlet in zincblende-type CdS. This effect had not been seen in the earlier measurements on cubic and hexagonal ZnS, since the E_1 peak of this material is masked by the E_0' peak which does not split for wurtzite. The F_1 peak of hexagonal CdS, still unidentified in terms of transitions between energy bands, is absent in cubic CdS, thus confirming the earlier contention that this peak is characteristic of wurtzite-type crystals.

We shall summarize now, for future reference, the general features of the reflection spectra of zincblende-type crystals. A peak, sometimes very weak, is generally seen near the lowest direct absorption edge E_0, due to transitions between predominantly p-like wave functions of the anion (Γ_{15} symmetry) and s-like functions of the cation (Γ_1). This peak exhibits the spin-orbit splitting of the Γ_{15} state. At higher energies, one sees the E_1 peak, due to direct transitions at a $\mathbf{k}$ point in the [111] direction inside the Brillouin zone, between a state of Λ_3 symmetry and a state of Λ_1 symmetry. This peak displays the spin-orbit splitting of the Λ_3 state, which is also predominantly p-like. In materials of low average atomic number (GaP, ZnS, CuCl, BP) the E_1 peak is replaced or masked by the E_0' peak, which is caused by transitions between the Γ_{15} valence band state (predominantly p-like) of the anion and another Γ_{15} state (predominantly p-like) of the cation. At higher energies, the E_2 peak appears. It is due to transitions at the [100] edge of the zone ($X_5 \rightarrow X_1$, $X_5 \rightarrow X_3$) and in the [110] direction inside the zone ($\Sigma_4 \rightarrow \Sigma_1$). This peak shows a number of components due to its various contributions. Next in energy, the E_1' peak appears. This peak is due to $L_3 \rightarrow L_3$ transitions for $\mathbf{k}$ in the [111] direction at the edge of the zone, and hence also shows spin-orbit splitting. The d_1 peak, possibly due to $L_3 \rightarrow L_1$ transitions,[4] is seen at higher energies and finally the d_2 peak, due to transitions from core d-electron levels of the cation to unidentified conduction band states.

Peaks due to transitions at $\mathbf{k}=0$ change little when going from zincblende to wurtzite. Peaks due to transitions at a Λ or L point ([111] direction) split because of the inequivalent nature of the [111] direction of zincblende, which becomes the c axis of wurtzite, and the [111] direction, which becomes a low symmetry direction in wurtzite. Such splitting, and its corresponding

* Supported by the Advanced Research Projects Agency and the National Science Foundation.
† Supported by the Energetics Branch of the U. S. Air Force Cambridge Research Laboratory under Contract No. AF 19(628)-2845.
[1] M. Cardona, *Proceedings of the International Conference on the Physics of Semiconductors, Paris 1964* (Dunod Cie., Paris, 1964), p. 181.
[2] M. Cardona, Phys. Rev. **129**, 1068 (1963).
[3] J. Birman, Phys. Rev. **115**, 1493 (1959).
[4] J. C. Phillips, Phys. Rev. **133**, A452 (1964).

polarization selection rules, have been observed for the E_1 peak of CdS and CdSe.[5]

PREPARATION AND EPITAXY OF CdS MODIFICATIONS FOR REFLECTIVITY MEASUREMENTS

Epitaxial growth of CdS on {111}GaAs and GaP single-crystal slices and naturally grown platelets has been accomplished by chemical reaction vapor-phase transport techniques. HCl-H_2 mixtures have been employed as transport media. Good growth was obtained at temperatures between 710 and 730°C, with an optimum temperature of 720°C. The temperature was kept constant within ±1.5°C.

In the case of CdS deposition from H_2-HCl mixtures, specular hexagonal layers were deposited on the cation side of both materials; however, faceted pseudo-cubic (3*R*-rhombohedral) deposits were observed on the anion faces of the GaAs and GaP substrates. The existence of these modifications was verified by light figure and x-ray analysis.[6] Since the angle between the rhombohedral axis of the pseudo-cubic layers[6] is close to 60°, we call them "cubic" throughout this paper.

Perfect epitaxy was observed in all hexagonal overgrowths, i.e., {00.1} parallel to {111}, with the cation face of both, host and epitaxial layer, always pointing in identical directions. In some cases, perfect epitaxy was also observed in pseudo-cubic CdS deposition on the {1$\bar{1}$1} "P-face" of GaP. In many cases, as a consequence of lattice misfit, symmetrical and slightly misoriented epitaxial layers of pseudocubic CdS were observed on GaAs and GaP substrates.

The nucleation of the two CdS structures formed on opposite crystal faces of the two substrates may be explained as follows: The formation of the stable, hexagonal modification can be interpreted by heterogeneous two-dimensional nucleation. No propagation mechanism through screw dislocations can be assumed in this case, as the stacking sequence of substrate (3*C* zincblende structure of 30 stacking in Zhdanov notation) and deposit (2*H* wurtzite structure of 11 stacking) differ markedly. Propagation of structure and stacking order from the substrate via screw dislocations originating in the latter is, however, a possible mechanism of formation of the metastable CdS epitaxial deposit of pseudocubic structure (3*R* of 30 stacking). The induction of the proper stacking of the various CdS layers in 3*R*–30 zincblende-type sequence may be further aided by a favorable combination of the chemistry of deposition and the {1$\bar{1}$1} crystal-face geometry. This may be elaborated as follows: Let us assume that the stability of the 2*H* wurtzite structure (as compared to 3*C* zincblende structure stability) is largely caused by relatively strong ionic interaction[7] between third nearest neighbors of opposite electronic charge which are separated by a distance $(1-u)\mathbf{c}$ in the *c* direction; here $u\mathbf{c}$ represents the unit translation parameter correlating the anionic and cationic hcp sublattices of the wurtzite structure. On the {111} cation face of the substrate, sulfur atoms then attach themselves to gallium atoms of the uppermost atomic layer of the substrate surface; next, cadmium atoms which follow subsequently attach themselves to the sulfur atoms in a (wurtzite-type) position nearest to, and directly above, the phosphorus or arsenic atoms of the second atomic layer of the substrate surface. In this way, a minimum (electrostatic) interface energy results. This process of S-Cd double layer deposition indefinitely repeats in identical fashion, now representing ordinary CdS crystal growth in [001] direction.

On the opposite {1$\bar{1}$1} "As"—or "P"—surface of the substrate, on the other hand, a different process takes place. Cadmium atoms of $CdCl_2$ molecules of the vapor phase ($CdS+2HCl \rightleftharpoons CdCl_2+H_2S$) attach themselves to arsenic or phosphorus atoms of the uppermost atomic layers of the substrate surface, while the two (still attached) chlorine atoms of the $CdCl_2$ molecule position themselves in (wurtzite-type) arrangements opposite, above, and nearest to, the gallium atoms of the second atomic layer of the substrate. This arrangement is electrostatically most favorable. Possibly, the remaining tetrahedral bonding site at the cadmium atoms may also be occupied by HCl from the gas phase. The first CdS double layer can then only be completed by interlinking the cadmium atoms with sulfur atoms locating themselves at the remaining "interstitial" tetrahedral sphalerite-type sites, while simultaneously releasing the chlorine atoms. The first CdS atomic double layer of zincblende stacking (with respect to the substrate) has thus formed. Subsequently, there are two possibilities that either (1) the process is indefinitely repeated, thus producing zincblende-type pseudocubic (rhombohedral) CdS (in this case, pseudocubic CdS could be grown from HCl–$CdCl_2$–H_2S gas phase directly on the {00.1} face of hexagonal CdS) or else (2) the stacking sequence first formed is further perpetuated by screw dislocations initiated by the existing substrate-overgrowth misfit. Both mechanisms, however objectionable for any specific reasons, gain in credibility in view of the fact that sparse, minute sections of hexagonal structure, as identified by optical microscopy and light figure reflections, tend to diminish in size through pseudo-cubic overgrowth. Also, the fact that the CdS etch morphology, as obtained in gaseous and aqueous HCl media, definitely points to the surface stabilization of CdS through the attachment of chlorine

[5] M. Cardona and G. Harbeke, Phys. Rev. **137**, A1465 (1965).
[6] M. Weinstein, G. A. Wolff, and B. N. Das, Appl. Phys. Letters **6**, 73 (1965).

[7] High ionicity in materials of tetrahedral coordination is generally considered a factor favoring wurtzite over zincblende structure.

atoms to the Cd surface atoms, lends further credence to the model discussed.[8]

REFLECTIVITY MEASUREMENTS

The measurements were performed with a MacPherson 1-m Seya-Namioka monochromator by the technique described earlier.[9] Most of the measurements were performed at room temperature. An attempt was made to resolve the exciton structure at E_0 at liquid-nitrogen temperature,[10] but no appreciable sharpening of this structure was observed. This is not surprising, in view of the inhomogeneous lateral strain associated with the mismatch between the host crystal and the epitaxial layer and the other crystal imperfections present. Hence E_0 exciton studies cannot differentiate between the cubic or hexagonal nature of our crystals.

As indicated in the previous section, the cubic phase of CdS only grows on the $\{1\bar{1}1\}$ anion face of the cubic substrates. On the cation face, a shiny specular deposit of the hexagonal material is obtained. The cubic deposit is dull in appearance, due to the presence of crystal facets, and yields a smaller specular reflectance. Hence measurements on the cubic and hexagonal deposited faces of the same slab are possible. These measurements demonstrate in a striking way the similarities and differences between the optical properties of both crystal structures.

The hexagonal sides of our samples have a long-wavelength specular reflectance close to that calculated from the refractive index.[11] The reflectivity of the cubic side is only about $\frac{1}{10}$ of the value expected for a specular surface. However, since this appears to be due to the presence of crystal facets on the surface and not the roughness on a microscopic scale, we believe that the reflection spectrum characteristic of a perfect flat surface is obtained by scaling all reflectivities so as to obtain good agreement with the long-wavelength reflectivity calculated from the refractive index.[11]

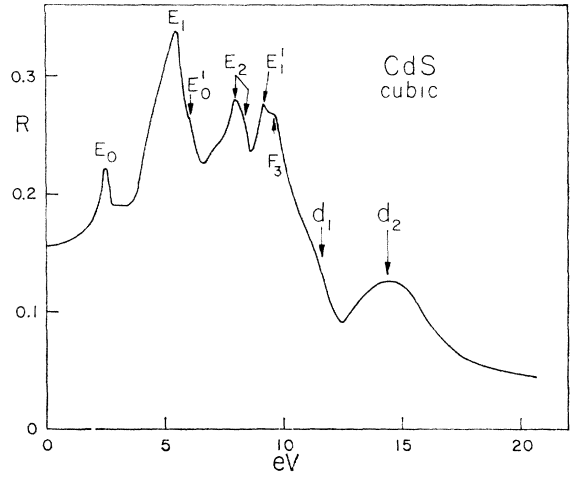

FIG. 1. Reflection spectrum at room temperature of a cubic CdS layer deposited on the arsenic face of GaAs.

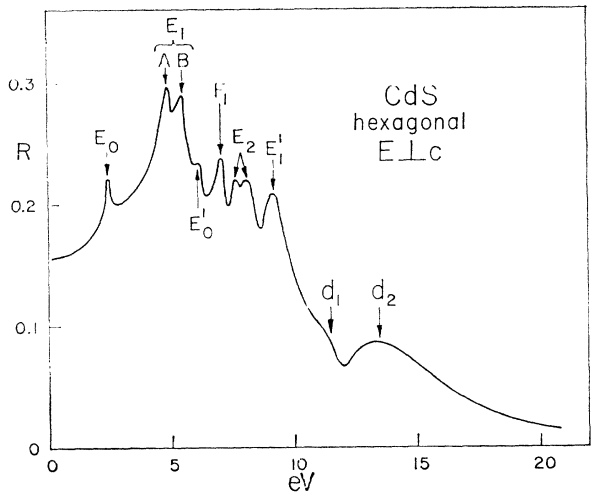

FIG. 2. Reflection spectrum at room temperature of a hexagonal CdS layer deposited on the gallium face of GaAs.

RESULTS AND DISCUSSION

The room-temperature reflectivity spectrum of a cubic and a hexagonal layer of CdS deposited epitaxially on the "As face" and "Ga face" of a {111} GaAs slab is shown in Figs. 1 and 2. The E_1 peak, which has two components A and B for the hexagonal layer, has only one component for the cubic layer. Similarly, the F_1 peak, characteristic of wurtzite-type spectra,[5] is almost completely absent for the cubic phase (some remains of F_1 may be indicative of a small amount of wurtzite admixture). No significant differences are seen between the E_0, E_0', E_2, E_1', d_1, and d_2 peaks of the cubic and the hexagonal phases. Similar results have been reported[5] for ZnS, but for this material the striking E_1 effects are not seen, since this peak is covered by the stronger E_0' peak. Figure 3 shows the real (ϵ_1) and imaginary (ϵ_2) parts of the dielectric constant of cubic CdS obtained from the Kramers-Kronig analysis of the reflection data.[5] The position of the various peaks observed in the reflectivity R and in ϵ_2 at room temperature is listed in Table I. For the sake of completeness, we have also listed the peaks observed in bulk hexagonal CdS.[5] Figure 4 shows the absorption coefficient α calculated from the data of Fig. 3. The fundamental absorption edge E_0 levels off at 2.55 eV and hence agrees within the accuracy of our Kramers-Kronig analysis with the leveling off point of the corresponding edge of hexagonal CdS (2.55 eV).[12] A somewhat more accurate idea of

[8] G. A. Wolff, J. J. Frawley, and J. R. Hietanen, J. Electrochem. Soc. **111**, 22 (1964).
[9] M. Cardona and D. L. Greenaway, Phys. Rev. **131**, 98 (1963).
[10] D. G. Thomas and J. J. Hopfield, Phys. Rev. **116**, 573 (1959).
[11] T. M. Bieniewski and S. J. Czyzak, J. Opt. Soc. Am. **53**, 494 (1963).
[12] D. Dutton, Phys. Rev. **112**, 785 (1958).

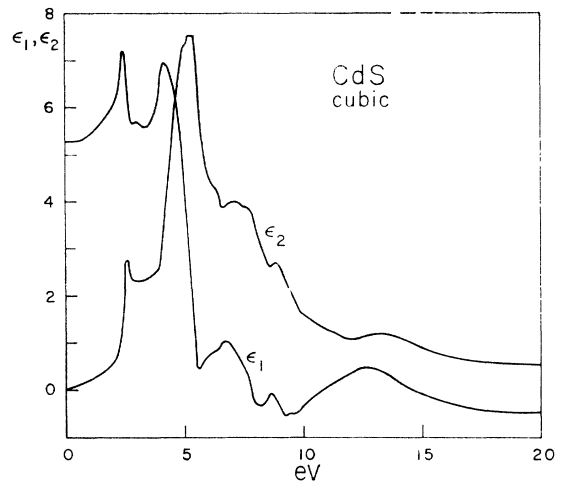

FIG. 3. Real (ϵ_1) and imaginary (ϵ_2) parts of the dielectric constant of cubic CdS obtained by the Kramers-Kronig analysis of the data of Fig. 1.

the differences in E_0 between bulk hexagonal CdS and our epitaxial layers can be obtained by direct comparison of the photon energy at which the E_0 reflection peak occurs. We find this peak at room temperature at somewhat lower energies for the epitaxial layers (cubic 2.50 eV, hexagonal 2.46 eV) than for bulk hexagonal material (2.53 eV).[5] This decrease in gap is, no doubt, produced by the imperfect nature of our epitaxial layers: Shifts in energy gaps towards lower energies with increasing concentration of lattice defects have been reported for many materials.[13] Since these shifts need not be the same for the cubic as for the hexagonal epitaxial samples, we cannot reach any quantitative conclusion about the energy difference between cubic and hexagonal CdS other than that the E_0 gaps differ by less than 0.1 eV (gap shifts with defects larger than 0.1 eV are not likely). The E_0 gaps of cubic ZnS [14] and ZnSe [15] are 0.1 eV smaller than the gaps of the corresponding hexagonal materials.

TABLE I. Peaks in the reflection spectrum (R) and in the imaginary part of the dielectric constant (ϵ_2) observed at room temperature in epitaxial CdS (cubic and hexagonal) and in bulk hexagonal CdS.

		CdS Bulk hexagonal $E\perp C$	CdS Epitaxial hexagonal $E\perp C$	CdS Epitaxial cubic
E_0	R	2.53	2.46	2.50
	ϵ_2	2.55	2.55	2.55
E_0'	R	6.1	6.15	6.20
	ϵ_2	6.1	6.15	6.4
$E_1(A)$	R	4.93	4.88	forbidden
	ϵ_2	4.9	4.95	
$E_1(B)$	R	5.50	5.47	5.49
	ϵ_2	5.4	5.45	5.3
E_2	R	8.0, 8.35	7.67, 8.18	7.95
	ϵ_2	7.55	7.7, 8.1	7.5
E_1'	R	9.15	9.18	9.18
	ϵ_2	8.85	9.15	8.8
d_1	R		11.6	11.9
	ϵ_2			11.6
d_2	R	14.0	13.4	14.4
	ϵ_2	13.0	12	13.3
F_1	R	7.12	7.07	forbidden
	ϵ_2	7.0	7.05	
F_3[a]	R	9.8		9.7
	ϵ_2	9.6		9.6

[a] Reference 5.

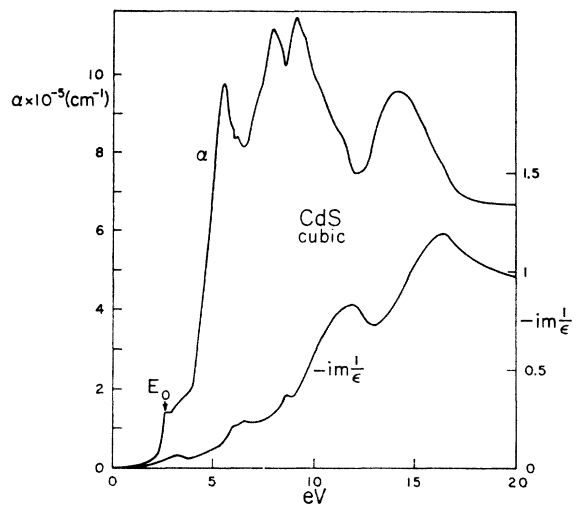

FIG. 4. Absorption coefficient (α) and energy loss function $[-\mathrm{Im}(1/\epsilon)]$ of cubic CdS derived from the data of Fig. 3.

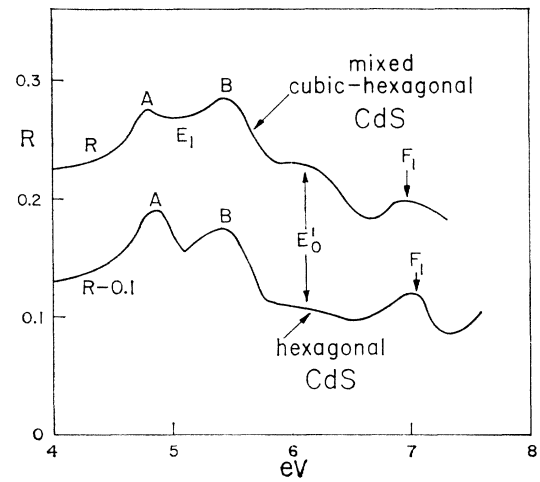

FIG. 5. Reflection spectrum at room temperature of a hexagonal CdS layer deposited on the gallium face of GaP and a mixed cubic-hexagonal CdS layer deposited on the phosphorus face of GaP.

[13] J. I. Pankove and P. Aigrain, Phys. Rev. **126**, 956 (1962).

[14] J. A. Beun and G. T. Goldsmith, Helv. Phys. Acta **33**, 508 (1960).

[15] Y. S. Park and F. L. Chan, J. Appl. Phys. **36**, 800 (1965).

The energy-loss function[16] $-\mathrm{Im}(1/\epsilon)$ of our cubic CdS is also seen in Fig. 4. The peaks of this function correspond to plasma resonances. The peak at 16.4 eV correspond to the plasma resonance of the valence electrons, somewhat modified by the presence of interband transitions originating at the d electrons of the cation. A strong secondary resonance is seen at 11.8 eV. Similar effects have been reported[17] for hexagonal CdS.

The reflection spectrum of the hexagonal CdS deposited on the gallium side of the GaAs substrate shown in Fig. 2 agrees reasonably well with that of bulk hexagonal CdS. In particular, the splitting of E_1 into the $A-B$ doublet and the appearance of the F_1 peak is clearly seen. However, small shifts towards lower energies by about 0.05 eV are seen for the peaks E_0, E_1, E_0', and F_1. These shifts could be due to strains or imperfections. The E_2 peaks seem to have shifted by a larger amount ($\sim$0.2 eV) towards lower energies with respect to those of bulk hexagonal CdS.

Figure 5 shows a section of the reflection spectrum of partially cubic CdS, deposited on the $\{1\bar{1}1\}$ "P face" of GaP, and that of pure hexagonal CdS deposited on the opposite "Ga face." It is seen that the intensity of the A and F_1 peaks is lower for the partially cubic material. Hence a clear indication of the mixed structure of this CdS layer, which is difficult to obtain from x-ray data, is readily obtained from reflectivity measurements. By using the epitaxial deposition technique one should, therefore, be able to obtain optical data for the metastable phases of many III–V, II–VI, and I–VII materials.

[16] H. R. Philipp and H. Ehrenreich, Phys. Rev. **129**, 1550 (1963).

[17] M. Balkanski and Y. Petroff, *Proceedings of the International Conference on the Physics of Semiconductors, Paris 1964* (Dunod Cie, Paris, 1964).

PHYSICAL REVIEW VOLUME 140, NUMBER 2A 18 OCTOBER 1965

Theory of Phonon-Assisted Tunneling in Semiconductors*†

LEONARD KLEINMAN
Department of Physics, University of Southern California, Los Angeles, California
(Received 30 November 1964)

We calculate the phonon-assisted tunneling current for a model p-n junction (as opposed to the homogeneous-electric-field model) due to two mechanisms. A first-order mechanism in which an electron on, say, the p side scatters to a state on the n side with the emission of a phonon yields results similar to those calculated by other workers for the homogeneous-electric-field model and is about three orders of magnitude too small to account for the experimentally observed current. A second-order process in which an electron on the p side tunnels to an intermediate state in a higher band on the n side via the interband term in the Hamiltonian and then scatters with the emission of a phonon to a final state on the n side yields a current equal in magnitude to the experimentally observed current. This mechanism also succeeds, where the first one fails, in accounting for the magnitude of an differences between the experimentally measured pressure coefficients π_{LA}^+, π_{LA}^-, π_{TA}^+, π_{TA}^- where $\pi=J^{-1}dJ/dP$, the superscripts identify the direction of current flow, and the subscripts, the branch of the phonon involved in the tunneling process (LA=longitudinal acoustic, TA=transverse acoustic).

I. INTRODUCTION

THE theory of direct and phonon-assisted indirect tunneling in semiconductors has been developed for the homogeneous-electric-field case by Keldysh[1] and Kane[2] and applied to the heavily doped Esaki[3] p-n junction by Kane.[4] Fredkin and Wannier[5] (hereafter FW) have developed the theory of direct tunneling for a model p-n junction with a constant electric field in the intermediate region and zero field on both the p and n sides. Price and Radcliffe[6] have discussed the p-n junction with position-dependent electric field. FW's work essentially confirms Kane's result. The success of the homogeneous-field model in explaining direct tunneling in p-n junctions is at first sight surprising since in a constant electric field each electron wave function consists of a superposition of all the Bloch functions in the band with a fixed $\mathbf{k}_\perp$, the component of wave vector perpendicular to the electric field. However, it may be understood for the following reasons: (1) Because the tunneling matrix element [Eq. (7) of Ref. 2] depends

* A large portion of this research was accomplished while the author was at the University of Pennsylvania and was there supported by the Advanced Research Projects Agency.

† This work was supported in part by the Joint Services Electronics Programs (U. S. Army, U. S. Navy, and U. S. Air Force) under Contract No. AF-AFOSR-496-64.

[1] L. V. Keldysh, Zh. Eksperim. i Teor. Fiz. **33**, 994 (1957); **34**, 962 (1958) [English transls.: Soviet Phys.—JETP **6**, 763 (1958); **7**, 665 (1958)].

[2] E. O. Kane, J. Phys. Chem. Solids **12**, 181 (1959).

[3] L. Esaki, Phys. Rev. **109**, 603 (1958).

[4] E. O. Kane, J. Appl. Phys. **32**, 83 (1961).

[5] D. R. Fredkin and G. H. Wannier, Phys. Rev. **128**, 2054 (1962).

[6] P. J. Price and J. M. Radcliffe, IBM J. Research Develop. **3**, 364 (1959).